

A spartan model for the LHC diphoton excess

Thomas Appelquist,^a James Ingoldby,^a Maurizio Piai,^b Jedidiah Thompson.^a

^a*Department of Physics, Sloane Laboratory, Yale University, New Haven, Connecticut 06520, USA*

^b*Department of Physics, College of Science, Swansea University, Singleton Park, SA2 8PP, Swansea, Wales, UK*

ABSTRACT: We propose a simple model accommodating the reported 750 GeV diphoton excess seen in the first 13-TeV run of the LHC. It leads to testable predictions, in particular for di-lepton production, at higher integrated luminosity. We append to the minimal standard model a new gauge sector with its own $SU(2)$ symmetry group. A new complex doublet scalar field provides mass for the new vectors and describes the 750-GeV resonance. An adequate rate for the diphoton signals, with resonant production via photon fusion, requires the VEV of the new scalar field to be somewhat less than the electroweak scale. This in turn requires the new heavy vectors to have sub-TeV masses and be strongly coupled. A new global $U(1)$ symmetry plays a key role. Current precision-electroweak constraints are respected.

Contents

1	Introduction	1
2	The Model	2
3	Precision Electroweak and Higgs physics	5
4	Heavy Scalar Resonance	7
4.1	Tree-level ZZ Decay	7
4.2	Loop-induced Decays	8
4.3	H Production and Parameter Estimates	9
5	Vector resonances	10
5.1	Neutral Vector	10
5.2	Charged Vectors	11
6	Symmetry and fine tuning	12
7	Summary and Outlook	13
A	Parton Distribution Functions	14

1 Introduction

Hints of new physics beyond the standard model (SM) continue to emerge from the LHC. From the recent run at 13 TeV, the ATLAS and CMS collaborations have reported an excess in the diphoton mass distribution at about 750 GeV, with a statistical significance of $2 - 4\sigma$ [1]. The current data is compatible both with a very narrow resonance, and with a resonance of width $\mathcal{O}(50\text{ GeV})$. Our analysis here favors the first option. We present a simple model, developed as an effective field theory (EFT), that accommodates these signals, is consistent with existing SM tests, and makes predictions that could be testable soon at the LHC. The main ingredient is an extension of the SM gauge sector with the addition of a new, spontaneously broken $SU(2)$ gauge group.

In models with generic $SU(2)$ extensions of the SM gauge sector, indirect bounds from precision measurements of electroweak and Higgs physics tend to favor the regime of weakly-coupled vectors in the multi-TeV mass range (see for instance [2] and references therein). Here we employ a simple model, designed to focus on the 750-GeV diphoton signal and associated physics, which allows for sub-TeV masses for the new vectors and is consistent with precision electroweak and Higgs measurements (see also [3]).

We describe the Higgs and gauge sectors of the minimal SM using a complex doublet Φ with vacuum expectation value (VEV) f . We include a new $SU(2)_V$ gauge sector and a new complex-doublet field Φ_V with VEV f_V to provide mass for the three $SU(2)_V$ gauge bosons. The field Φ_V transforms as a bi-fundamental under $SU(2)_R \times SU(2)_V$, where the diagonal T^3 generator of $SU(2)_R$ is electroweak gauged. After symmetry breaking, the residual massive scalar H coming from Φ_V is our candidate for the 750 GeV resonance. The fermionic field content of the model is that of the SM. The full field content of the model is shown in Table 1.

With respect to other models in the recent literature [4], ours has a distinctive combination of features. It has an accidental, approximate global $U(1)$ symmetry, which emerges together with a simple mechanism responsible for suppressing new contributions to electroweak precision observables. Indirect bounds from electroweak and Higgs physics are satisfied despite the presence of new sub-TeV vector and scalar particles. The dominant production process for the new narrow heavy scalar particle H is photon fusion [5]. Since there are no new, fermionic degrees of freedom, the coupling of the heavy scalar particle H to photons is dominated by loops of the new vector bosons.

In Section 2 we describe the model in detail, and in Section 3 we discuss Higgs physics and electroweak precision constraints. We discuss the properties of the H resonance in Section 4, estimating its decay width and production cross section at the LHC. We conclude that $f_V \lesssim f$. In Section 5 we estimate the production and decays of the new, heavy vector states and conclude that the $SU(2)_V$ gauge coupling must be relatively strong to make the vector states heavy enough to have avoided detection. Nevertheless, production estimates indicate that these states should be accessible in future LHC runs. We will comment on the predictive power of the EFT in the relevant range of parameters. In Section 6 we describe the symmetry properties of our model and the issue of fine tuning. We summarize our results in Section 7 and describe possible extensions of our study.

2 The Model

The field content of our model is listed in Table 1. The hypercharge Y of the matter fields is given by $Y = T_R^3 + \frac{1}{2}(B - L)$, where T_R^3 is the diagonal generator of $SU(2)_R$. We also write $B_\mu \equiv B_\mu^3 [T_R^3 + \frac{1}{2}(B - L)]$, while $W_\mu = W_\mu^a T^a$ and $V_\mu = V_\mu^a T^a$, so that all gauge-boson fields are written as 2×2 matrices. We normalize the T^a generators of $SU(2)$ by $\text{Tr } T^a T^b = \frac{1}{2} \delta^{ab}$. The Lagrangian, including operators up to dimension-four, is

$$\begin{aligned} \mathcal{L} = & +2g \text{Tr } W^\mu J_{L\mu} - 2g' \text{Tr } B^\mu J_{Y\mu} & (2.1) \\ & - \frac{1}{2} \text{Tr } W_{\mu\nu} W^{\mu\nu} - \frac{1}{2} \text{Tr } V_{\mu\nu} V^{\mu\nu} - \frac{1}{2} \text{Tr } B_{\mu\nu} B^{\mu\nu} \\ & + \frac{1}{4} \text{Tr } |D\Phi|^2 + \frac{1}{4} \text{Tr } |D\Phi_V|^2 - V(\Phi_i) \\ & - \frac{1}{\sqrt{2}} \bar{q}_L \Phi y_q q_R - \frac{1}{\sqrt{2}} \bar{\ell}_L \Phi y_\ell \ell_R, \end{aligned}$$

with y_q and y_ℓ being $SU(2)_R$ -breaking Yukawa matrices that will give rise to the masses of the SM fermions in the familiar way. The field strength tensors are defined so that the

		$SU(2)_L$	Φ	$SU(2)_R$	Φ_V	$SU(2)_V$	
		$SU(2)_L$		$U(1)_Y$		$SU(2)_V$	
Fields		$SU(2)_L$	$SU(2)_R$	$SU(2)_V$	$U(1)_{B-L}$	$U(1)_Y$	
Φ	2		$\bar{2}$	1	0	$\pm 1/2$	
Φ_V	1		2	$\bar{2}$	0	$\mp 1/2$	
q_L	2		1	1	$1/3$	$1/6$	
q_R	1		2	1	$1/3$	$1/6 \pm 1/2$	
ℓ_L	2		1	1	-1	- $1/2$	
ℓ_R	1		2	1	-1	$-1/2 \pm 1/2$	
W_μ	3		1	1	0	0	
V_μ	1		1	3	0	0	
B_μ	1		*	1	0	0	

Table 1. The field content of the model. The figure shows a diagrammatic representation of the model, with the global (top) and local (bottom) symmetries acting on the scalars Φ and Φ_V made manifest. All fermions q_i and ℓ_i are written as Weyl spinors, and all vectors are written as 2×2 matrices (see main text for details).

gauge bosons are canonically normalized. We denote with g , g' and g_V the three gauge couplings. $J_{L\mu}$ and $J_{Y\mu}$ are electroweak matter currents bilinear in the SM fermion fields. The covariant derivatives for the scalars are

$$D_\mu \Phi \equiv \partial_\mu \Phi - i(gW_\mu \Phi - g'B_\mu \Phi) ,$$

$$D_\mu \Phi_V \equiv \partial_\mu \Phi_V - i(g'V_\mu \Phi_V - g_V \Phi_V V_\mu) .$$

We write the potential with the same conventions as in [2]:

$$V(\Phi_i) = +\frac{\lambda}{16} \left(\text{Tr} \left[\Phi \Phi^\dagger - f^2 \mathbb{I}_2 \right] \right)^2 + \frac{\lambda_V}{16} \left(\text{Tr} \left[\Phi_V \Phi_V^\dagger - f_V^2 \mathbb{I}_2 \right] \right)^2 . \quad (2.2)$$

We have omitted the dimension-four mixing term $\text{Tr}(\Phi \Phi^\dagger) \text{Tr}(\Phi_V \Phi_V^\dagger) = 2 \text{Tr}(\Phi \Phi_V \Phi_V^\dagger \Phi^\dagger)$. The only communication between Φ and Φ_V then arises via the weakly-coupled gauge field B_μ . In Section 6 we will justify the omission of the mixing term by observing that with a TeV-scale cutoff for our EFT, it will be generated at the loop level, but with a very small coefficient. Minimization of the potential yields the VEVs $\langle \Phi \rangle = f \mathbb{I}_2$ and $\langle \Phi_V \rangle = f_V \mathbb{I}_2$.

In the absence of the weakly-coupled gauge field B_μ , the global $SU(2)_R$ transformation can act independently on Φ and Φ_V . In effect, it splits into two $SU(2)$'s. The gauging via B_μ couples these two, leaving an extra $U(1)_V$ global symmetry in addition to the gauged symmetries. Among the gauged symmetries, the unbroken $U(1)_Q$ of QED is generated by $Q = T_L^3 + Y + T_V^3$. The additional global $U(1)_V$ can be taken to be

$$U(1)_V : (\Phi_V(x), V_\mu(x)) \rightarrow e^{i\beta_V T^3} (\Phi_V(x), V_\mu(x)) e^{-i\beta_V T^3} , \quad (2.3)$$

where β_V is a real number. The $U(1)_V$ symmetry, preserved even in the presence of a mixing term in the potential, stabilizes the charged V_μ^\pm . This symmetry can and will be broken, allowing for decay of the charged vector. The breaking will arise from unknown physics at a high scale Λ_V , and will be communicated to our fields by higher-dimension operators suppressed by powers of Λ_V .¹ The neutral V_μ^0 mixes with the Z_μ via the B_μ gauge interaction.

The 2×2 mass matrix \mathcal{M}_+^2 for the charged vectors, in the (W^μ, V^μ) basis, is

$$\mathcal{M}_+^2 = \frac{1}{4} \begin{pmatrix} g^2 f^2 & 0 \\ 0 & g_V^2 f_V^2 \end{pmatrix}. \quad (2.4)$$

Since there is no mixing in the charged sector, we have

$$g_{\text{SM}} = g, \quad v_W = f, \quad (2.5)$$

where $v_W \simeq 246$ GeV is the electroweak scale and $g_{\text{SM}} \simeq 0.65$ is the $SU(2)_L$ coupling in the SM.

The 3×3 mass matrix for the neutral vector bosons in the basis (W^μ, B^μ, V^μ) is

$$\mathcal{M}_0^2 = \frac{1}{4} \begin{pmatrix} g^2 f^2 & -g g' f^2 & 0 \\ -g g' f^2 & g'^2 (f^2 + f_V^2) & -g' g_V f_V^2 \\ 0 & -g' g_V f_V^2 & g_V^2 f_V^2 \end{pmatrix}. \quad (2.6)$$

The diagonalization of this mass matrix yields a massless photon, along with the Z_μ and a heavy V_μ^0 vector, with masses

$$M_{Z,V^0}^2 = \frac{1}{8} \left\{ f^2 (g^2 + g'^2) + f_V^2 (g'^2 + g_V^2) \right. \\ \left. \pm \sqrt{f^4 (g^2 + g'^2)^2 - 2f^2 f_V^2 (g_V^2 (g^2 + g'^2) + g'^2 (g - g')(g + g')) + f_V^4 (g'^2 + g_V^2)^2} \right\}. \quad (2.7)$$

To ensure that $M_{V^0}^2 \gg M_Z^2$, the term $f_V^4 (g'^2 + g_V^2)^2$ must dominate in the square root. To describe the properties of the 750 GeV scalar, we will find it necessary to keep $f_V \lesssim f$, and therefore we will take $g_V^2 \gg g^2, g'^2$. In this limit,

$$M_Z^2 \simeq \frac{1}{4} (g^2 + g'^2) f^2 - \frac{1}{4} \frac{g'^4}{g_V^2} f^2 + \dots, \quad (2.8)$$

$$M_{V^0}^2 \simeq \frac{1}{4} (g_V^2 + g'^2) f_V^2 + \frac{1}{4} \frac{g'^4}{g_V^2} f^2 + \dots. \quad (2.9)$$

The eigenstate of the photon A_μ is

$$A_\mu = \frac{1}{\sqrt{g^2 g_V^2 + g'^2 g^2 + g'^2 g_V^2}} \left(g_V g' W_\mu^3 + g_V g B_\mu + g g' V_\mu^3 \right). \quad (2.10)$$

¹ Equivalently, one can think of symmetry breaking as arising in the UV completion via small symmetry breaking terms, without the need to introduce a parametrically large scale Λ_V .

The analogous expressions for the heavy vectors Z_μ and V_μ^0 are more complicated, but can be approximated for $g^2, g'^2 \ll g_V^2$ as

$$Z_\mu \simeq \frac{g}{\sqrt{g^2 + g'^2}} W_\mu^3 - \frac{g'}{\sqrt{g^2 + g'^2}} B_\mu - \frac{g'}{g_V} \frac{g'}{\sqrt{g^2 + g'^2}} V_\mu^3, \quad (2.11)$$

$$V_\mu^0 \simeq V_\mu^3 - \frac{g'}{g_V} B_\mu, \quad (2.12)$$

where we have neglected terms of $\mathcal{O}(g^2/g_V^2)$ and of $\mathcal{O}(g'^2/g_V^2)$.

The electric charge is given by

$$e \equiv \frac{gg'g_V}{\sqrt{g^2g'^2 + g'^2g_V^2 + g^2g_V^2}}. \quad (2.13)$$

Then, with the electroweak $U(1)$ gauge coupling defined to be

$$g'_{\text{SM}} = \frac{g'g_V}{\sqrt{g_V^2 + g'^2}}, \quad (2.14)$$

we have the conventional relation $e = g'_{\text{SM}} g_{\text{SM}} / \sqrt{g'_{\text{SM}}^2 + g_{\text{SM}}^2}$. From here on, we take $g_V^2 \gg g^2, g'^2$ in all expressions. Then, $g' \simeq g'_{\text{SM}} \simeq 0.36$.

The masses of the two physical scalars are obtained by writing $\Phi = (f + h)\mathbb{I}_2$ and $\Phi_V = (f_V + H)\mathbb{I}_2$, and are given by

$$m_h^2 = 2\lambda f^2, \quad m_H^2 = 2\lambda_V f_V^2. \quad (2.15)$$

For $m_h = 125$ GeV we have $\lambda \simeq 0.13$, while $m_H = 750$ GeV and $f_V \lesssim f$ require $\lambda_V \gtrsim 9/2$. We make this estimate more precise when considering the properties of the 750 GeV scalar.

3 Precision Electroweak and Higgs physics

The new sector of our model communicates with the SM fields only through the B_μ gauge field with strength g' . The new particles are heavy relative to the SM particles by virtue of the fact that $g_V^2 \gg g^2, g'^2$ and $\lambda_V \gg \lambda$. On the other hand, with masses below 1 TeV, the new particles are light enough to raise concerns about their impact on electroweak precision studies. Deviations from the SM are captured in a set of electroweak precision parameters [6, 7], related to a set of local operators, which arise from integrating out the heavy physics, at tree-level and loop-level. The local operators are to be used at tree level along with loop effects arising from SM particles. The leading parameters and associated operators through dimension-six are tabulated in [7].

At low energies the new physics in our model leads only to local, gauge invariant operators constructed from the B_μ field. Here we focus on operators contributing to the electroweak precision observables. The dimension-four operator is $\text{Tr } B_{\mu\nu} B^{\mu\nu}$, re-scaling a term already in the Lagrangian. At tree level the single dimension-six operator, arising

from mixing with the heavy sector is $\text{Tr}(\partial_\sigma B_{\mu\nu})(\partial^\sigma B^{\mu\nu})$. It affects only the neutral-vector-boson two-point function and corresponds directly to the Y parameter of Ref. [7]. A simple tree-level calculation in the limit $g_V^2 \gg g^2, g'^2$ yields

$$Y \simeq \frac{g'^2 g^2 f^2}{g_V^4 f_V^2} = \frac{g'^2 M_W^2}{g_V^2 M_{V^\pm}^2}, \quad (3.1)$$

exhibiting both mass and mixing suppression. According to [7], the bound on Y is $|Y| < 0.0006$ (at 1σ c. l.). This translates into the mild bound $g_V M_{V^\pm} \gtrsim 1$ TeV, which is well respected by our model. In the limit $g_V \rightarrow \mathcal{O}(4\pi)$, this estimate becomes very small, but should be regarded as order-of-magnitude since higher order corrections can become important.

The other precision parameters of Ref. [7], in particular the \hat{S} parameter, are not generated in our model until we enlarge it to include new Lagrangian terms suppressed by a very high-scale (see Section 6). We will take these terms to violate the $U(1)_V$ symmetry in order to allow for decay of the V_μ^\pm bosons. They will make very small contributions to the precision electroweak parameters.²

Some of the couplings of the Higgs particle h have been measured precisely enough that they can also be a source of concern for models of new physics [2, 8]. In our model, because of the $U(1)_V$ symmetry, the couplings of h to the fermions and to charged W bosons are identical to those of the SM. Hence there are no tree-level corrections to the process $h \rightarrow WW$ and no sizeable corrections to the loop-induced $h \rightarrow \gamma\gamma$. However, the tree-level coupling of h to Z_μ bosons is modified by the effect of mixing in the neutral sector between the photon, Z_μ and V_μ^0 . The experimental bounds coming from the $h \rightarrow ZZ^*$ process [8], can be written in terms of the signal significance as $\mu_{ZZ} = 1.31_{-0.24}^{+0.27}$ (1σ c.l.). We exhibit the coupling by writing $\Phi = (f + h)\mathbb{I}_2$, giving an interaction of the form

$$\mathcal{L}_h = \frac{h}{f} \sum_{i,j} V_i^\mu (M_i a_{hij} M_j) V_{j\mu}, \quad (3.3)$$

where $V_i = (Z, V^0)$ and $M_i = (M_Z, M_{V^0})$. In the large- g_V limit, the 2×2 interaction matrix reads:

$$a_{hij} = \begin{pmatrix} 1 - \frac{g'^4 f^2}{g_V^4 f_V^2} & \frac{g'^2 f}{g_V^2 f_V} \\ \frac{g'^2 f}{g_V^2 f_V} & \frac{g'^4 f^2}{g_V^4 f_V^2} \end{pmatrix}, \quad (3.4)$$

where again we have kept only the leading terms in the $1/g_V^2$ expansion. As the $h \rightarrow ZZ^*$ branching ratio is small, and the h production mechanism is unaffected, we can approximate

²With the other precision parameters vanishing, the Y parameter is related simply to the ρ parameter via $\Delta\rho \equiv \rho - 1 = Y g'^2/g^2$ [7]. Thus, in the limit $g_V^2 \gg g^2, g'^2$, at the tree level we would have

$$\Delta\rho \equiv \frac{M_W^2}{M_Z^2} \frac{g'^2 + g^2}{g^2} - 1 \approx \frac{g'^4 f^2}{g_V^4 f_V^2} + \dots \quad (3.2)$$

$\mu_{ZZ} \simeq a_{hZZ}^2 \mu_{ZZ}^{\text{SM}}$. Together with the experimental bound quoted earlier, this allows us to conclude that at the 3σ level

$$a_{hZZ}^2 \simeq 1 - 2 \frac{g'^4 f^2}{g_V^4 f_V^2} \gtrsim 0.6. \quad (3.5)$$

Because of the small deviation from the SM, suppressed by factors $\mathcal{O}(g'^4/g_V^4)$ (the same order as the precision Y parameter), this constraint is easily satisfied.

4 Heavy Scalar Resonance

We identify H with the heavy particle seen in diphoton searches at 750 GeV [1]. We borrow the conventions of [9], and write the production cross-section as

$$\sigma(pp \rightarrow H \rightarrow \gamma\gamma) = \frac{1}{M_H \Gamma_H s} \left[\sum_i C_{ij} \Gamma(H \rightarrow ij) \right] \Gamma(H \rightarrow \gamma\gamma), \quad (4.1)$$

where $\sqrt{s} = 13$ TeV, and where the sum is over all the partons in the initial state, including the photon. The partonic luminosities C_{ij} are discussed in the Appendix. In order to reproduce the experimental excesses, it may be necessary for cross sections to be as large as $\sigma \simeq (4.8 \pm 2.1)$ fb (CMS) and $\sigma \simeq (5.5 \pm 1.5)$ fb (ATLAS) [10]. We estimate the parameters of our model required to provide cross sections in this range, or somewhat smaller given that the signals are preliminary.

We assume that the masses of the V^i bosons are large enough to forbid decays of H into final states involving these bosons. As noted earlier, this will be achieved by taking $f_V \lesssim f$ and $g_V^2 \gg g^2, g'^2$. The quantum number assignments are such that H cannot decay directly to two fermions, as only Φ enters the Yukawa couplings and there is no mixing between H and h . The absence of mixing in the charged vector-boson sector, a consequence of the $U(1)_V$ symmetry of the dimension-four Lagrangian, ensures that H cannot decay to W -boson pairs.³ The requirement $M_{V^0} = g_V f_V / 2 \gtrsim 660$ GeV forbids the decay $H \rightarrow V^0 Z^0$. Thus, the only allowed decays are $H \rightarrow \gamma\gamma, \gamma Z, ZZ$. The latter can proceed at the tree level while all three can proceed at the quantum level via loops of charged V_μ^\pm vector bosons. The production process is dominated by photon fusion via the same loops.

4.1 Tree-level ZZ Decay

As with the Higgs scalar h , we write the couplings of H to the neutral vector-boson mass eigenstates by writing $\Phi_V = (f_V + H)\mathbb{1}_2$, so that the Lagrangian contains a coupling

$$\mathcal{L}_H = \frac{H}{f_V} \sum_{i,j} V_i^\mu (M_i a_{Hij} M_j) V_{j\mu}, \quad (4.2)$$

³Both of these conclusions are altered by small mixing effects between h and H and by even smaller $U(1)_V$ symmetry breaking couplings, discussed later in the paper. Both of these give highly suppressed contributions to the width of the H .

where $V_i = (Z, V^0)$ and $M_i = (M_Z, M_{V^0})$. For large g_V , the mixing matrix reads:

$$a_{Hij} = \begin{pmatrix} \frac{g'^4 f^2}{g_V^4 f_V^2} & -\frac{g'^2 f}{g_V^2 f_V} \\ -\frac{g'^2 f}{g_V^2 f_V} & 1 - \frac{g'^4 f^2}{g_V^4 f_V^2} \end{pmatrix}. \quad (4.3)$$

By unitarity, $a_h + a_H = \mathbb{I}_2$.

The decay rate, adapted from the analogous SM decay of a heavy Higgs particle [11], reads

$$\Gamma(H \rightarrow ZZ) = a_{HZZ}^2 \frac{m_H^3}{32\pi f_V^2} \sqrt{1-4x} \left(1 - 4x + 12x^2 \right), \quad (4.4)$$

where $x = M_Z^2/m_H^2$. Here, with $x \ll 1$ and with

$$a_{HZZ} \simeq \frac{g'^4 M_W^2}{g^2 g_V^2 M_{V^\pm}^2}, \quad (4.5)$$

we have

$$\Gamma^{\text{tree}} \simeq a_{HZZ}^2 \frac{m_H^3}{32\pi f_V^2} = \frac{g'^8 M_W^4 m_H^3}{32\pi g^4 g_V^4 M_{V^\pm}^4 f_V^2}. \quad (4.6)$$

For $g_V^2 \gg g^2, g'^2$, the requisite mixing renders the width very small. As we discuss in Section 6, a comparable contribution to the amplitude will come from the small mixing between H and h arising at the loop level. Both are dominated by loop contributions that do not suffer from such strong mixing suppression.

4.2 Loop-induced Decays

The coupling of H to two photons is controlled by a dimension-five operator generated by loops of charged particles. Because of the simple structure of the model, the only one-loop contribution comes from the V_μ^\pm , as no fermions couple to H . Adapting the decay rate of the Higgs boson to photons in the SM to the present case [11], we have

$$\Gamma(H \rightarrow \gamma\gamma) = \left(\frac{v_W}{f_V} \right)^2 \frac{G_F \alpha^2 m_H^3}{128\sqrt{2}\pi^3} \left| A_W \left(\frac{m_H^2}{4M_{V^\pm}^2} \right) \right|^2, \quad (4.7)$$

where

$$A_W(x) = -\frac{1}{x^2} \left(2x^2 + 3x + 3(2x-1)\arcsin^2 \sqrt{x} \right). \quad (4.8)$$

The appearance of v_W is for convenience. It is cancelled by the factor G_F , leaving only scales associated with the new sector. In the limit $x \ll 1$, relevant to the present case, one finds $A_W \left(\frac{m_H^2}{4M_{V^\pm}^2} \right) \rightarrow -7$, and we have

$$\Gamma(H \rightarrow \gamma\gamma) \simeq 3 \text{ MeV} \left(\frac{v_W}{f_V} \right)^2. \quad (4.9)$$

The loop-induced decays to ZZ and $Z\gamma$, in the limit $M_Z \ll m_H$, are obtained in the same manner. Neglecting the tree-level contribution to the decay to ZZ , the one-loop expressions (for $g_V^2 \gg g^2, g'^2$) are

$$\Gamma(H \rightarrow Z\gamma) = 2 \left(\frac{g'}{g} \right)^2 \Gamma(H \rightarrow \gamma\gamma) \simeq 0.61 \Gamma(H \rightarrow \gamma\gamma), \quad (4.10)$$

$$\Gamma(H \rightarrow ZZ) = \left(\frac{g'}{g} \right)^4 \Gamma(H \rightarrow \gamma\gamma) \simeq 0.09 \Gamma(H \rightarrow \gamma\gamma). \quad (4.11)$$

The one-loop two-body decay widths together yield

$$\Gamma^{\text{tot}} \simeq \frac{(g^2 + g'^2)^2}{g^4} \Gamma(H \rightarrow \gamma\gamma) \simeq 1.71 \Gamma(H \rightarrow \gamma\gamma) \simeq 5 \text{ MeV} \left(\frac{v_W}{f_V} \right)^2, \quad (4.12)$$

giving a relatively narrow width and a large diphoton branching ratio $\text{BR}_{\gamma\gamma}$ in the relevant range of parameter space.

4.3 H Production and Parameter Estimates

Production proceeds via photon fusion. The expression for the $\gamma\gamma$ production cross section is

$$\sigma(pp \rightarrow H \rightarrow \gamma\gamma) = \frac{\text{BR}_{\gamma\gamma}}{M_H s} C_{\gamma\gamma} \Gamma(H \rightarrow \gamma\gamma) \simeq 0.5 \text{ fb} \left(\frac{v_W}{f_V} \right)^2 \text{BR}_{\gamma\gamma}, \quad (4.13)$$

where $\sqrt{s} = 13$ TeV.

With the large value of $\text{BR}_{\gamma\gamma}$ implied by Eq. (4.12), this expression can approach the level indicated by the experimental signals in diphoton searches, but only if f_V is no larger than v_W . If the estimates following Eq. (4.1) are accurate, f_V might have to be as low as ~ 100 GeV, giving a production cross section times branching ratio of ~ 2 fb. On the other hand, if smaller cross sections are eventually revealed, then we could have $f_V \sim v_W$. These estimates are affected by large uncertainties in the partonic luminosity $C_{\gamma\gamma}$ (see the Appendix). Because the total width is small, our model can accommodate the hints of new resonant production only in terms of a single, narrow-width resonance.

If f_V must be as low as 100 GeV, then $g_V^2 = 4M_V^2/f_V^2 \rightarrow \mathcal{O}(16\pi^2)$ and $\lambda_V = 2M_H^2/f_V^2 \rightarrow \mathcal{O}(16\pi^2)$. The new sector in our model becomes strongly coupled, raising the question of whether it truly functions as an EFT, capturing all the relevant degrees of freedom and allowing for reliable approximate computations. If not, our one-loop estimates for the decay widths and branching ratios of the new scalar H should be regarded as order-of-magnitude estimates. The same is true of our estimates of the precision electroweak parameters, but they were comfortably small due to mixing and mass suppression.

If it develops that the production cross section Eq. (4.1) is small enough to allow $f_V \sim v_W$, then $g_V^2, \lambda_V < (4\pi)^2$, and perturbation theory could become reliable. The cutoff on the EFT, to be discussed in Section 6, would be somewhat above the masses of the new scalar and vectors, perhaps in the few-TeV range. Our model would function as a bona fide EFT over a limited energy range. Either way, the model provides a plausible explanation for a 750 GeV resonance with a large branching ratio to photons.

5 Vector resonances

With parameters in the range described above, V_μ^0 and V_μ^\pm are approximately degenerate and have masses in the range of the diphoton resonance H .

5.1 Neutral Vector

The neutral vector is produced and decays dominantly via tree-level processes, induced by the mixing between B_μ , W_μ^3 and V_μ^0 . We write the general LHC production cross-section as in [9]:

$$\sigma(pp \rightarrow V^0 \rightarrow X) = \frac{3}{M_{V^0} \Gamma_{V^0} s} \left[\sum_{ij} C_{ij} \Gamma(V^0 \rightarrow ij) \right] \Gamma(V^0 \rightarrow X). \quad (5.1)$$

The relevant parton luminosities C_{ij} are the quark-antiquark ones (see Appendix A).

The dominant contributions to the decay rates come from two-body final states, which for kinematical reasons involve only SM particles. Because of the large mass of the V_μ^0 , we approximate the rates by ignoring the masses of the final state particles.

We write the effective couplings to the fermions as

$$\mathcal{L} = \frac{g'}{g_V} g' V_\mu^0 J_Y^\mu + \mathcal{O}\left(\frac{1}{g_V^2}\right) \quad (5.2)$$

where J_Y^μ is the $U(1)_Y$ current made of fermions. We then obtain:

$$\Gamma(V^0 \rightarrow u\bar{u}) = \frac{17}{288\pi} \frac{g'^4}{g_V^2} M_{V^0}, \quad (5.3)$$

$$\Gamma(V^0 \rightarrow d\bar{d}) = \frac{5}{288\pi} \frac{g'^4}{g_V^2} M_{V^0}, \quad (5.4)$$

$$\Gamma(V^0 \rightarrow e^+e^-) = \frac{5}{96\pi} \frac{g'^4}{g_V^2} M_{V^0}, \quad (5.5)$$

$$\Gamma(V^0 \rightarrow \nu_e \bar{\nu}_e) = \frac{1}{96\pi} \frac{g'^4}{g_V^2} M_{V^0}. \quad (5.6)$$

The total width for decay to three families of fermions, treating them all as massless, is

$$\Gamma(V^0 \rightarrow \psi\bar{\psi}) = \frac{5}{12\pi} \frac{g'^4}{g_V^2} M_{V^0}. \quad (5.7)$$

The decay to SM bosons (WW and Zh) yields a smaller contribution to the total width:

$$\Gamma(V^0 \rightarrow W^+W^-) \simeq \Gamma(V^0 \rightarrow Zh) \simeq \frac{1}{192\pi} \frac{g'^4}{g_V^2} M_{V^0}. \quad (5.8)$$

We conclude that the branching ratio to electron-positron is $\text{BR}(V^0 \rightarrow e^+e^-) \simeq \frac{1}{8}$. Taking $g' \simeq 0.36$, $g_V \lesssim 4\pi$ and making the representative choice $M_{V^0} \simeq 700$ GeV, we find that

the predicted LHC production cross-sections for e^+e^- and $\mu^+\mu^-$ (collectively denoted by $\ell^+\ell^-$) are:

$$\sigma(pp \rightarrow V^0 \rightarrow \ell^+\ell^-)_{8\text{TeV}} \simeq (21000 \text{fb}) \frac{g'^4}{g_V^2} \gtrsim 2 \text{fb}, \quad (5.9)$$

$$\sigma(pp \rightarrow V^0 \rightarrow \ell^+\ell^-)_{13\text{TeV}} \simeq (53000 \text{fb}) \frac{g'^4}{g_V^2} \gtrsim 6 \text{fb}, \quad (5.10)$$

at $\sqrt{s} = 8$ TeV and 13 TeV, respectively. The explicit dependence on M_{V^0} drops from the cross-section, but it re-enters through the PDF, evaluated at the scale M_{V^0} . For indicative choices of parameters relevant to our study, the width is $\Gamma \simeq \mathcal{O}(10 \text{ MeV})$.

From the LHC run at 8 TeV, the upper bound on the above cross section from ATLAS [12] for $M_{V^0} \simeq 700$ GeV is $\sigma(pp \rightarrow V^0 \rightarrow \ell^+\ell^-) \lesssim 2 \text{ fb}$. In the 13 TeV case [13] it is $\sigma(pp \rightarrow V^0 \rightarrow \ell^+\ell^-) \lesssim 7 \text{ fb}$ ⁴. In the limit $g_V \rightarrow 4\pi$, the bounds appear to be satisfied, although the estimates should be viewed as order-of-magnitude due to strong coupling as discussed in Section 4.3. For the case $g_V^2 < (4\pi)^2$, corresponding to $f_V \sim v_W$, the estimates appear to be at or somewhat above the published experimental bounds. However, the combination of experimental error and uncertainties in our theoretical estimates associated, for example, with the M_{V^0} -dependence of the parton distribution functions, leaves open the possibility that our predictions remain compatible with current upper bounds.

These estimates offer the exciting possibility that with higher integrated luminosity the production and decay of the V_μ^0 should be observable. It should be possible to test the viability of the current model by looking for di-lepton excesses with an invariant mass comparable to m_H at the LHC.

5.2 Charged Vectors

In the charged sector, the presence of the g' coupling does not lead to mixing with the SM gauge bosons. The charged V_μ^\pm is stable due to the $U(1)_V$ symmetry necessarily present in the dimension-four Lagrangian. When higher-dimension terms are added, however, this symmetry is easily broken. A simple example is the dimension-six operator

$$\frac{1}{\Lambda_V^2} \text{Tr} \left[(D_\mu \Phi) \Phi_V (D^\mu \Phi_V)^\dagger \Phi^\dagger \right], \quad (5.11)$$

which can lead, for example, to the decay $V^\pm \rightarrow W^\pm h$. The scale Λ_V at which the $U(1)_V$ symmetry is broken must be large enough so that operators of this type lead to only small corrections to the precision quantities discussed in Section 3. Conversely, the scale must be small enough to ensure that the V^\pm decays rapidly enough to avoid direct detection. The broad range $1 \text{ TeV} \ll \Lambda_V \lesssim 1000 \text{ TeV}$ will allow both constraints to be easily satisfied.

The production cross-section for the V_μ^\pm is dominated by pair production mediated by a virtual γ_μ , Z_μ or V_μ^0 . The cross section is suppressed with respect to the V_μ^0 production cross-section, in part because the parton luminosities are smaller at the higher energies

⁴The bounds quoted here are computed from the experimental data by assuming that the candidate heavy vector has the branching ratios of an SM Z boson but with a mass of 700 GeV.

needed to produce on-shell pairs V_μ^\pm . Also the final states of the decays are more difficult to reconstruct. We conclude that these processes are less likely to yield important future signals than processes involving the V_μ^0 .

6 Symmetry and fine tuning

Our model has the following features.

- At the dimension-four level, before gauging and neglecting Yukawa couplings, the model possesses a global $SU(2)^4$ symmetry. (The $SU(2)_R$ symmetry in Table 1 can act independently on the new sector and the SM sector.) This symmetry is present even when including all possible terms in the dimension-four potential, including the sector-coupling term $\text{Tr}(\Phi\Phi^\dagger)\text{Tr}(\Phi_V\Phi_V^\dagger) = 2\text{Tr}(\Phi\Phi_V\Phi_V^\dagger\Phi^\dagger)$, neglected so far.
- The $SU(2)^4$ symmetry is explicitly broken by the gauging of an $SU(2)_L \times U(1)_Y \times SU(2)_V$ subgroup, preserving an additional, accidental, global $U(1)_V$ symmetry. At the dimension-four level, communication between the new sector and the SM fields is via the gauging of the hypercharge Y , controlled by the small coupling g' .
- The fermionic field content, charge assignments and dimension-four Yukawa interactions are chosen in such a way so as to preserve the same symmetry, and to reproduce the SM at low energies.
- The $U(1)_V$ accidental symmetry, which stabilizes the V_μ^\pm , is broken only by higher-dimension operators such as the one in (5.11), suppressed by a very high scale Λ_V .
- The self-coupling of Φ_V and the gauge coupling of $SU(2)_V$ are much larger than the electroweak couplings, possibly reaching the non-perturbative limit $\lambda_V, g_V^2 \rightarrow (4\pi)^2$.

We next discuss corrections to the scalar potential, which has not included the mixing term between Φ and Φ_V , and the issue of fine tuning. The one-loop effective potential, arising from the gauge bosons only, can be written in terms of the cutoff scale Λ and renormalization scale μ as

$$\begin{aligned} V_1 = & \frac{3\Lambda^2}{256\pi^2} \left[(3g^2 + g'^2) \text{Tr} \Phi^\dagger \Phi + (g'^2 + 3g_V^2) \text{Tr} \Phi_V^\dagger \Phi_V \right] + \\ & + \frac{3}{4096\pi^2} \left[(3g^4 + 2g^2 g'^2 + g'^4) (\text{Tr} \Phi^\dagger \Phi)^2 + 2g'^4 (\text{Tr} \Phi^\dagger \Phi) (\text{Tr} \Phi_V \Phi_V^\dagger) \right. \\ & \left. + (g'^4 + 2g'^2 g_V^2 + 3g_V^4) (\text{Tr} \Phi_V \Phi_V^\dagger)^2 \right] \ln \frac{\mu^2}{\Lambda^2} + \dots, \end{aligned} \quad (6.1)$$

In addition, there are Λ^2 and $\ln \Lambda^2$ terms arising from the scalar self-couplings and from the fermion Yukawa couplings. We omit them for simplicity.

Consider first the terms quadratic in the cutoff, which contribute to the masses of h and H . The $\text{Tr}(\Phi\Phi^\dagger)$ term (including additional contributions from the Higgs self coupling and top-quark Yukawa coupling) will not require substantial fine tuning as long as Λ is less than a few TeV. The $\text{Tr}(\Phi_V\Phi_V^\dagger)$ term has a contribution proportional to g_V^2 , as well as to λ_V (not

shown). Again, the cutoff can be no larger than a few TeV to avoid substantial fine tuning of the mass m_H . With g_V and λ_V approaching the strong coupling limit, this estimate is only order-of-magnitude. Interestingly, with the top loop dominating the $\text{Tr}(\Phi\Phi^\dagger)$ term, it has the opposite sign of the one-loop $\text{Tr}(\Phi_V\Phi_V^\dagger)$ term.

At the $\ln\Lambda^2$ level, the $(\text{Tr}\Phi_V\Phi_V^\dagger)^2$ term can be of the same order of magnitude as the corresponding tree-level term if g_V^2 and λ_V approach the strong-coupling level. There is no fine-tuning issue here, although once again the estimates are order-of-magnitude in the strong coupling limit. The $(\text{Tr}\Phi\Phi^\dagger)^2$ term is smaller.

The mixing term, which is proportional to only g'^4 , is the smallest of the $\ln\Lambda^2$ terms since $g'^4 \ll g^4 \ll g_V^4$. Although it breaks no symmetries and is dimension-four, it leads to only small mixing effects between the Higgs field h and the heavy scalar H , and can consistently be neglected to leading approximation.

Finally, we note again that each of the allowed dimension-four terms in our Lagrangian, (including the mixing term) necessarily respects the global $U(1)_V$ symmetry. Since this accidental symmetry stabilizes the V_μ^\pm bosons, we have invoked new $U(1)_V$ -breaking interactions at a very high scale $\Lambda_V \gg \Lambda$, described by higher-dimension operators, to allow them to decay. An example is given in Eq. (5.11). These higher-dimension operators can contribute to each of the electroweak parameters, but since the associated scale is very high, their contribution will be very small.

7 Summary and Outlook

We have proposed a simple model describing the CMS and ATLAS diphoton excess at 750 GeV. The new resonance is interpreted as a narrow scalar particle H associated with the mechanism for the spontaneous breaking of a new $SU(2)_V$ gauge symmetry. Thus, the model predicts the existence of three heavy vectors V_μ^i . Their masses are required to be large enough to avoid direct decay of H into final states including the new vectors.

The model yields a $\mathcal{O}(1\text{ fb})$ cross-section at the LHC for the resonant production of H via photon fusion with the coupling of H to photons induced by loops of charged vector bosons. To make the coupling to photons strong enough to provide a sufficiently large production cross section, f_V can be taken no larger than the electroweak scale. It is therefore necessary to have a large gauge coupling g_V , so as to make the new vectors sufficiently massive.

All the indirect bounds from precision electroweak and Higgs physics are satisfied despite the comparatively low masses of the new particles and their large self-interactions. We have highlighted the special features of the model leading to this property, as well as the intrinsic uncertainties in our estimates. The model is directly testable, as at least the neutral V_μ^0 has a production cross-section and branching ratios large enough to be detectable via its leptonic decays in higher-luminosity runs of the LHC.

In the event that the signals of H are confirmed, and that hints of a new V_μ^0 resonance emerge, two related lines of enquiry are suggested by this study. First, the rich and model-dependent phenomenology of the charged V_μ^\pm should be explored further, as it depends sensitively on the $U(1)_V$ -violating operators responsible for its finite lifetime. Second, the

simplicity of our EFT leaves open many possibilities for its UV completion, but the relatively strong coupling of its new sector indicates that the completion lies nearby in energy. Since our new sector is not responsible for electroweak symmetry breaking, we envisage the UV completion to have properties very different from technicolor-like models. Whatever its nature, we anticipate new states appearing just above the TeV scale, where they should be experimentally accessible.

Acknowledgments

We thank Yang Bai, Luigi Del Debbio and Sarah Demers for helpful discussions. The work of TA and JI is supported by the U.S. Department of Energy under the contract DE-FG02-92ER-40704. The work of MP is supported in part by the STFC Consolidated Grant ST/L000369/1.

A Parton Distribution Functions

To make predictions for the LHC, we use the PDFs from NNPDF [14, 15]. We define the dimensionless parton luminosities with the same conventions as in [9]:

$$C_{q\bar{q}} \equiv \frac{4\pi^2}{9} \int_{M^2/s}^1 \frac{dx}{x} \left[q(x) \bar{q} \left(\frac{M^2}{x s} \right) + \bar{q}(x) q \left(\frac{M^2}{x s} \right) \right], \quad (\text{A.1})$$

$$C_{gg} \equiv \frac{\pi^2}{8} \int_{M^2/s}^1 \frac{dx}{x} g(x) g \left(\frac{M^2}{x s} \right), \quad (\text{A.2})$$

$$C_{\gamma\gamma} \equiv 8\pi^2 \int_{M^2/s}^1 \frac{dx}{x} \gamma(x) \gamma \left(\frac{M^2}{x s} \right), \quad (\text{A.3})$$

where s is the Mandelstam variable and M the relevant scale of the process. We show in Table 2 and Fig. 1 the results for various choices of s and M .

We compared these to the parton luminosities from the MSTW [16] NLO package, and found excellent agreement for the quark and gluon luminosities. The agreement is at the few percent level, with the exception of the subdominant $b\bar{b}$, where it is at the 10% level. We also checked that the results we quote agree with [9].

The photon luminosity $C_{\gamma\gamma}$ determines the production cross section for the scalar H . It is given in Eq. (A.3) in terms of the photon PDFs, which have uncertainties ranging from 50% to 200% across the domain of the integral. There are also systematic uncertainties in the evolution of the photon PDFs by NNPDF. Alternative methods exist for the determination of $C_{\gamma\gamma}$, but a growing body of literature [17–19] indicates that the various methods agree on its order of magnitude. The combination of statistical and systematic uncertainties imply that the values we used for $C_{\gamma\gamma}$ (obtained from NNPDF) are affected by uncertainties as large as $C_{\gamma\gamma}$ itself.

\sqrt{s} (TeV)	M (GeV)	NNPDF						
		$C_{b\bar{b}}$	$C_{c\bar{c}}$	$C_{s\bar{s}}$	$C_{d\bar{d}}$	$C_{u\bar{u}}$	C_{gg}	$C_{\gamma\gamma}$
8	600.	3.5	8.4	18.	230.6	386.4	573.1	22.3
8	625.	2.8	6.7	14.5	194.9	328.0	459.1	19.6
8	650.	2.2	5.4	11.8	165.5	279.7	370.2	17.4
8	675.	1.8	4.3	9.6	141.1	239.5	300.2	15.4
8	700.	1.5	3.5	7.8	120.8	205.8	244.6	13.8
8	725.	1.2	2.9	6.4	103.8	177.5	200.3	12.3
8	750.	1.0	2.4	5.3	89.5	153.6	164.7	11.0
8	775.	0.8	1.9	4.4	77.4	133.3	136.2	9.9
8	800.	0.7	1.6	3.6	67.1	116.1	113.0	8.9
13	600.	44.1	100.5	189.2	1475.1	2351.8	6214.3	103.6
13	625.	36.2	82.7	157.0	1268.2	2031.4	5105.5	92.2
13	650.	29.9	68.4	131.0	1095.6	1762.9	4220.5	82.4
13	675.	24.9	56.9	109.8	950.7	1536.2	3507.8	73.9
13	700.	20.7	47.5	92.5	828.2	1343.9	2928.9	66.5
13	725.	17.4	39.9	78.2	724.2	1179.9	2457.5	60.0
13	750.	14.6	33.6	66.4	635.6	1039.4	2071.6	54.3
13	775.	12.4	28.4	56.6	559.7	918.6	1754.0	49.3
13	800.	10.5	24.1	48.4	494.5	814.3	1491.1	44.9

Table 2. Parton luminosities obtained from the NNPDF package [15] and the NNPDF23_nlo_as_0119_qed.LH grid, implementing QED and NLO QCD evolution with $\alpha_s(M_Z) = 0.119$ and $\alpha(M_Z) = 1/128$.

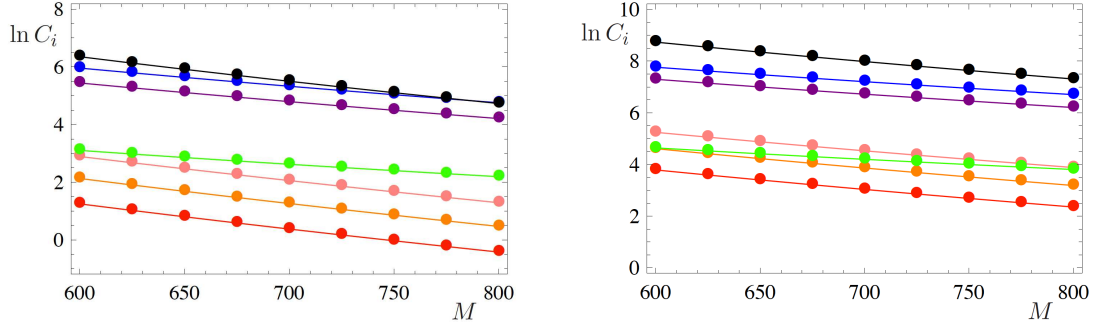


Figure 1. Central values for the parton luminosities from NNPDF, as a function of M (in GeV). The left panel has $\sqrt{s} = 8$ TeV, the right $\sqrt{s} = 13$ TeV. We show $C_{b\bar{b}}$ (red), $C_{c\bar{c}}$ (orange), $C_{s\bar{s}}$ (pink), $C_{d\bar{d}}$ (purple), $C_{u\bar{u}}$ (blue), C_{gg} (black) and $C_{\gamma\gamma}$ (green).

References

[1] The ATLAS collaboration, ATLAS-CONF-2015-081; CMS Collaboration, CMS-PAS-EXO-15-004.

- [2] T. Appelquist, Y. Bai, J. Ingoldby and M. Piai, arXiv:1511.05473 [hep-ph].
- [3] R. Casalbuoni, S. De Curtis and D. Dominici, Phys. Rev. D **70**, 055010 (2004) doi:10.1103/PhysRevD.70.055010 [hep-ph/0405188].
- [4] An incomplete list of models with an $SU(2)$ extension to the SM gauge group includes the following. W. C. Huang, Y. L. S. Tsai and T. C. Yuan, Nucl. Phys. B **909**, 122 (2016) doi:10.1016/j.nuclphysb.2016.05.002 [arXiv:1512.07268 [hep-ph]]; U. Aydemir and T. Mandal, arXiv:1601.06761 [hep-ph]; J. Ren and J. H. Yu, arXiv:1602.07708 [hep-ph]; H. Davoudiasl, P. P. Giardino and C. Zhang, arXiv:1605.00037 [hep-ph].
- [5] For discussions about photon fusion as a production mechanism for the 750 GeV resonance, see for example the following. C. Csáki, J. Hubisz and J. Terning, Phys. Rev. D **93**, no. 3, 035002 (2016) doi:10.1103/PhysRevD.93.035002 [arXiv:1512.05776 [hep-ph]]; J. de Blas, J. Santiago and R. Vega-Morales, arXiv:1512.07229 [hep-ph]; C. Csáki, J. Hubisz, S. Lombardo and J. Terning, arXiv:1601.00638 [hep-ph]. L. A. Harland-Lang, V. A. Khoze and M. G. Ryskin, JHEP **1603**, 182 (2016) doi:10.1007/JHEP03(2016)182 [arXiv:1601.07187 [hep-ph]]; S. I. Godunov, A. N. Rozanov, M. I. Vysotsky and E. V. Zhemchugov, arXiv:1602.02380 [hep-ph].
- [6] M. E. Peskin and T. Takeuchi, Phys. Rev. D **46**, 381 (1992). doi:10.1103/PhysRevD.46.381
- [7] R. Barbieri, A. Pomarol, R. Rattazzi and A. Strumia, Nucl. Phys. B **703**, 127 (2004) doi:10.1016/j.nuclphysb.2004.10.014 [hep-ph/0405040].
- [8] The ATLAS and CMS Collaborations, ATLAS-CONF-2015-044.
- [9] R. Franceschini *et al.*, arXiv:1512.04933 [hep-ph]; R. Franceschini, G. F. Giudice, J. F. Kamenik, M. McCullough, F. Riva, A. Strumia and R. Torre, arXiv:1604.06446 [hep-ph].
- [10] A. Strumia, arXiv:1605.090401 [hep-ph].
- [11] A. Djouadi, Phys. Rept. **457**, 1 (2008) doi:10.1016/j.physrep.2007.10.004 [hep-ph/0503172].
- [12] G. Aad *et al.* [ATLAS Collaboration], Phys. Rev. D **90**, no. 5, 052005 (2014) doi:10.1103/PhysRevD.90.052005 [arXiv:1405.4123 [hep-ex]].
- [13] The ATLAS collaboration, ATLAS-CONF-2015-070.
- [14] R. D. Ball *et al.* [NNPDF Collaboration], JHEP **1504**, 040 (2015) doi:10.1007/JHEP04(2015)040 [arXiv:1410.8849 [hep-ph]].
- [15] N. P. Hartland and E. R. Nocera, Nucl. Phys. Proc. Suppl. **234**, 54 (2013) doi:10.1016/j.nuclphysbps.2012.11.013 [arXiv:1209.2585 [hep-ph]];
- [16] A. D. Martin, W. J. Stirling, R. S. Thorne and G. Watt, Eur. Phys. J. C **63**, 189 (2009) doi:10.1140/epjc/s10052-009-1072-5 [arXiv:0901.0002 [hep-ph]].
- [17] A. D. Martin and M. G. Ryskin, Eur. Phys. J. C **74**, 3040 (2014) doi:10.1140/epjc/s10052-014-3040-y [arXiv:1406.2118 [hep-ph]].
- [18] C. Csáki, J. Hubisz and J. Terning, Phys. Rev. D **93**, no. 3, 035002 (2016) doi:10.1103/PhysRevD.93.035002 [arXiv:1512.05776 [hep-ph]].
- [19] S. Fichet, G. von Gersdorff and C. Royon, arXiv:1512.05751 [hep-ph].